

## Shell Model Calculation of the $\beta^-$ and $\beta^+$ Partial Half-Lives of $^{54}\text{Mn}$ and Other Unique Second Forbidden $\beta$ Decays

Gabriel Martínez-Pinedo<sup>1,2</sup> and Petr Vogel<sup>3</sup>

<sup>1</sup>*Institute of Physics and Astronomy, University of Århus, DK-8000 Århus, Denmark*

<sup>2</sup>*Kellogg Radiation Laboratory 106-38, California Institute of Technology, Pasadena, California 91125*

<sup>3</sup>*Department of Physics 161-33, California Institute of Technology, Pasadena, California 91125*

(Received 12 March 1998)

The nucleus  $^{54}\text{Mn}$ , observed in cosmic rays, decays there dominantly by the  $\beta^-$  branch with an unknown rate. The branching ratio of its  $\beta^+$  decay was determined recently. We use the shell model with only a minimal truncation and calculate both  $\beta^+$  and  $\beta^-$  decay rates. Good agreement for the  $\beta^+$  branch suggests that the calculated partial half-life of the  $\beta^-$  decay,  $4.94 \times 10^5$  yr, should be reliable. However, this half-life is noticeably shorter than the range  $1-2 \times 10^6$  yr indicated by the fit based on the  $^{54}\text{Mn}$  abundance in cosmic rays. We also evaluate other known unique second forbidden  $\beta$  decays from the  $p$  and  $sd$  shells and show that the shell model can describe them with reasonable accuracy as well. [S0031-9007(98)06562-4]

PACS numbers: 23.40.Hc, 21.60.Cs, 27.40.+z, 98.70.Sa

The nucleus  $^{54}\text{Mn}$  decays in the laboratory dominantly by electron capture to the  $2^+$  state in  $^{54}\text{Cr}$  with the half-life of 312 days. However, as a component of cosmic rays,  $^{54}\text{Mn}$  will be fully stripped of its atomic electrons, and this mode of decay is therefore impossible. The  $^{54}\text{Mn}$  nuclei were in fact detected in cosmic rays using the Ulysses spacecraft [1,2]. They offer an attractive possibility to use their measured abundance as a chronometer for the iron group nuclei (Sc–Ni) in cosmic rays in analogy to the chronometers based on the abundances of other long lived isotopes ( $^{10}\text{Be}$ ,  $^{26}\text{Al}$ , and  $^{36}\text{Cl}$ ). With them one can, in turn, determine the mean density of interstellar matter, a quantity of considerable interest. The use of the long lived nuclei as cosmic ray chronometers is reviewed in Ref. [3]. The importance of  $^{54}\text{Mn}$  for the understanding of propagation of the iron group nuclei that are products of explosive nuclear burning has been stressed in Refs. [4,5]. For this program to succeed, however, one must know the half-life of the stripped  $^{54}\text{Mn}$  ( $I^\pi = 3^+$ ). The decay scheme of  $^{54}\text{Mn}$  is shown in Fig. 1; the dashed lines indicate the decay paths of the stripped  $^{54}\text{Mn}$ .

In two recent difficult and elegant experiments the very small branching ratio for the  $\beta^+$  decay to the ground state of  $^{54}\text{Cr}$  has been measured:  $(2.2 \pm 0.9) \times 10^{-9}$  [6] and  $(1.20 \pm 0.26) \times 10^{-9}$  [7]. By taking the weighted mean of these values we extract the averaged branching ratio of  $(1.28 \pm 0.25) \times 10^{-9}$ . Combining it with the known half-life for  $^{54}\text{Mn}$  of 312.3(4) d [8], it corresponds to an experimental partial  $\beta^+$  half-life of  $(6.7 \pm 1.3) \times 10^8$  yr. As explained in [1,6,7] one expects, however, that the decay of the fully stripped  $^{54}\text{Mn}$  will be dominated by the at present unobservable  $\beta^-$  decay to the  $^{54}\text{Fe}$  ground state. Previously, the partial  $\beta^-$  half-life was estimated assuming that the  $\beta^-$  and  $\beta^+$  form factors are identical. Very recently, in Ref. [7], the ratio of the  $\beta^-$  and  $\beta^+$  form factors was calculated using a very truncated shell model and ex-

tending it by comparison with similar calculations in the  $sd$  shell. The estimated  $\beta^-$  half-life is  $(6.3 \pm 1.3) \times 10^5$  yr [7]. In this work we will use the state of the art shell model and evaluate not only the  $EC$  decay rate of the normal  $^{54}\text{Mn}$ , but also both decay branches of the unique second forbidden transitions  $^{54}\text{Mn}(3^+) \rightarrow ^{54}\text{Cr}(0^+)$  and  $^{54}\text{Mn}(3^+) \rightarrow ^{54}\text{Fe}(0^+)$ . By comparing the calculated  $\beta^+$  decay half-life (or branching ratio) to the measured one we hope to judge the reliability of the calculation. We then proceed to calculate the half-life of the unknown  $\beta^-$  decay.

The decays of stripped  $^{54}\text{Mn}$  are unique second forbidden transitions which depend on a single nuclear form factor (matrix element). Half-lives of several such decays in the  $p$  shell ( $^{10}\text{Be}$ ) and  $sd$  shell ( $^{22}\text{Na}$ , and two decay branches of  $^{26}\text{Al}$ ) are known and have been compared to the nuclear shell model predictions in Ref. [9]. For the  $sd$  shell nuclei, however, only calculations in a severely

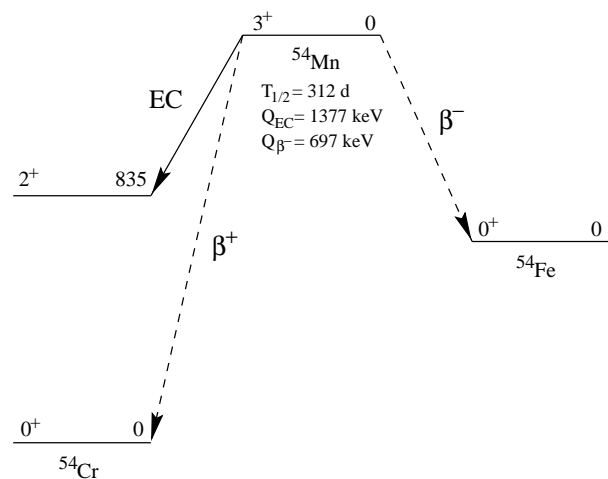


FIG. 1. Decay scheme of  $^{54}\text{Mn}$ .

truncated space were performed in [9]. Since that time computation techniques and programming skills have improved considerably. Thus, in order to further test our ability to describe this kind of weak decays, we repeat the analysis [9], using the exact shell model calculations without truncation. At the same time the availability of new (and different) experimental data for the  $^{10}\text{Be}$  [10] and  $^{26}\text{Al}$  [11] decays make necessary a new comparison between experiment and calculations.

In order to evaluate the decay rate we use the formulation of [12]. The number of particles with momentum  $p$  emitted per unit time is

$$N(p_e)dp_e = \frac{g^2}{2\pi^3} p_e^2 p_\nu^2 F(Z, W_e) C(W_e) dp_e, \quad (1)$$

where  $g$  is the weak coupling constant,  $p_e$  and  $W_e$  are electron (or positron) momentum and energy,  $p_\nu$  is the neutrino (or antineutrino) momentum, and  $Z$  is the atomic number of the daughter nucleus. All momenta and energies are in units where the electron mass is unity. For the Fermi function  $F(Z, W_e)$  we use the tabulated values, and the shape factor  $C(W_e)$  for the case of the unique second forbidden transitions is of the form

$$C(W_e) = \frac{R^4}{15^2} \left| {}^A F_{321}^{(0)} \right|^2 \left[ p_\nu^4 + \frac{10}{3} \lambda_2 p_\nu^2 p_e^2 + \lambda_3 p_e^4 \right]. \quad (2)$$

The nuclear form factor, in turn, is defined as

$${}^A F_{321}^{(0)} = g_A \sqrt{\frac{4\pi}{2J_i + 1}} \frac{\langle f | |r^2 [Y_2 \times \sigma]^{[3]} t_\pm | |i \rangle}{R^2}, \quad (3)$$

where  $i$  denotes the initial state and  $f$  the final one; the matrix element is reduced with respect to the spin space only (Racah convention [13]);  $\pm$  refers to  $\beta^\pm$  decay;  $t_\pm = (\tau_x \pm i\tau_y)/2$ , with  $t_+ p = n$ ;  $g_A = -1.2599 \pm 0.0025$  [14]; and  $R$  is the nuclear radius (the final expression for  $C(W_e)$  is obviously independent of  $R$ ).

The functions  $\lambda_2$  and  $\lambda_3$  are tabulated in [12]. Integrating the rate formula up to the spectrum end point we obtain the expression for  $1/\tau$  and, respectively, for the half-life [ $T_{1/2} = \ln(2)\tau$ ] in terms of the nuclear form factor squared. (For the stripped atoms we correct the end-point energy accordingly.) For the quantity  $2\pi^3(\ln 2)/g^2$  we use the value  $6146 \pm 6$  s [14]. Note the usual  $ft$  value, commonly used to characterize a decay, uses the integrated phase space factor  $f$  of Eq. (1)—however, without the constant  $g^2/2\pi^3 15^2$  and the radius factor  $R^4$ .

*Shell model calculations.*—In our calculation we consider an inert core of  $^{40}\text{Ca}$  with the 14 remaining nucleons distributed throughout the  $pf$  shell. We use KB3 [15] as the residual interaction with the single particle energies taken from the  $^{41}\text{Ca}$  experimental spectrum. The Hamiltonian is diagonalized with the code ANTOINE [16] using the Lanczos method. It is not yet possible to perform a full  $pf$ -shell calculation but we can come fairly close. Let's denote by  $f$  the  $f_{7/2}$  orbit and by  $r$  the rest of the  $pf$  shell

( $p_{3/2}$ ,  $p_{1/2}$ , and  $f_{5/2}$ ). From the calculations of Ref. [17] we know that one can get a good approximation to the results in the full  $pf$ -shell calculation when one considers the evolution of a given quantity as the number of particles  $n$  allowed to occupy the  $r$  orbits, increases. We have extended the calculations of the previous reference allowing up to a maximum of  $n = 7$  particles in the  $r$  orbits. The  $m$ -scheme dimensions for this calculation are 17 136 878 for  $^{54}\text{Cr}$ ; 49 302 582 for  $^{54}\text{Mn}$ ; 91 848 462 for  $^{54}\text{Fe}$ . Figure 2 shows the variation of the nuclear form factor for the  $\beta^+$  and  $\beta^-$  transitions as a function of the truncation level  $n$ . We have used the harmonic oscillator wave functions with  $b = 1.99$  fm. From Fig. 2 it is clear that our calculation has already converged for the  $n = 5$  truncation. It is also obvious that it would be inappropriate to use only the lowest order corrections ( $n = 2$  for  $\beta^-$  and  $n = 3$  for  $\beta^+$ ).

To see how well the calculated wave function reproduces basic characteristics of the ground state of the odd-odd nucleus  $^{54}\text{Mn}$ , note that the electric quadrupole moment is calculated to be  $Q = 34e \text{ fm}^2$  (with effective charges  $e_\pi = 1.5$  and  $e_\nu = 0.5$ ), while the experimental value is  $Q = 33 \pm 3e \text{ fm}^2$ . The magnetic moment, calculated with the free nucleon gyromagnetic factors is  $\mu = 2.78\mu_N$ , while the experimental value is  $\mu = (3.2819 \pm 0.0013)\mu_N$ . We have also calculated the  $\log ft$  value for the Gamow-Teller electron capture transition to the  $2^+$  state in  $^{54}\text{Cr}$ . The calculated  $\log ft = 6.14$ , where we have used the usual quenching factor of 0.76, is in good agreement with experimental value of 6.2. Note, however, that quenching of this allowed Gamow-Teller matrix element is needed to achieve the agreement with the experimental rate. (See [18] and references therein for the problem of the GT strength quenching.)

From Eq. (3) we know that the single particle matrix elements needed for the evaluation of the form factor involve the expectation value of  $r^2$  between the single-particle radial wave functions. In the evaluation of this quantity we have followed two approximations. First, we

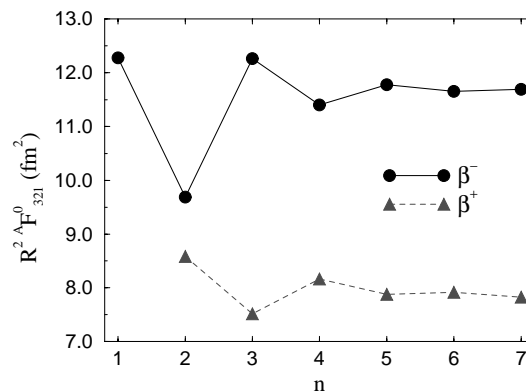


FIG. 2. Evolution of the matrix element  $R^2 A F_{321}^{(0)}$  with the truncation level  $n$ . The form factor has been evaluated using harmonic oscillator wave functions with  $b = 1.99$  fm.

consider harmonic oscillator wave functions. In this case all matrix elements are proportional to the square of the length parameter  $b$ . We use the prescription of Ref. [19] to determine  $b$  from the experimental charge radius  $\langle r^2 \rangle_{\text{ch}}^{1/2}$  [20] of the parent nucleus; this leads to  $b = 1.99$  fm in  $^{54}\text{Mn}$ . Second, we consider Woods-Saxon radial wave functions. They have been obtained using the potential well that includes spin-orbit and Coulomb terms [21]. The radial parameter of the well has been adjusted to reproduce the experimental charge radius. The values of the form factor and half-lives obtained using both methods are listed in Table I.

We have also evaluated the other known unique second-forbidden beta decays:  $^{10}\text{Be}(\beta^-)^{10}\text{B}$ ,  $^{22}\text{Na}(\beta^+)^{22}\text{Ne}$ , and  $^{26}\text{Al}(\beta^+)^{26}\text{Mg}$ . For the  $sd$ -shell nuclei we consider an inert core of  $^{16}\text{O}$  and the  $sd$  shell as the valence space. These transitions were previously computed in Ref. [9] using a truncated shell-model calculation. In our case, without truncating the  $sd$  shell space, we use the Wildenthal universal  $sd$ -shell (USD) effective interaction [22] and determine the radial parameters following the procedure outlined in the previous paragraph. In the harmonic oscillator approximation we use  $b = 1.78$  fm for  $^{22}\text{Na}$  and  $b = 1.81$  fm for  $^{26}\text{Al}$ . Table I contains the results of our calculations. For the decay of  $^{10}\text{Be}$  we reproduce the results of Ref. [9]; however, our determined  $b$  parameter, 1.75 fm, is slightly larger than the one used before ( $b = 1.68$  fm). The new experimental value for the half-life [10] nicely agrees with the computed one.

*Results and discussion.* — The top row of Table I shows that our shell model result agrees with the measured half-life of the  $\beta^+$  decay  $^{54}\text{Mn} \rightarrow ^{54}\text{Cr}$  within errors, without quenching of the corresponding form factor. The calculated  $\beta^-$  half-life,  $(4.94 \pm 0.06) \times 10^5$  yr (if we arbitrarily take the average value between HO and Wood-Saxon calculations), is noticeably shorter than the range expected in Refs. [1,2] ( $1-2 \times 10^6$  yr) based on the experimental abundance of  $^{54}\text{Mn}$  in cosmic rays and the model of the cosmic ray confinement.

Our calculation suggests that the form factor for the  $\beta^-$  decay,  $11.7$  fm $^2$ , is larger than the form factor for the  $\beta^+$

decay,  $7.8$  fm $^2$ . We can offer some intuitive, albeit very crude, understanding of this difference. Let us treat the three nuclei in the extreme single particle model. Also, instead of the actual transitions connecting the odd-odd nucleus  $^{54}\text{Mn}$  with the corresponding even-even ground state, let us consider the transitions from the seniority zero even-even nuclei to the odd-odd one. The  $\text{Cr} \rightarrow \text{Mn}$  transition would then involve  $(\pi f_{7/2})^4(\nu p_{3/2})^2 \rightarrow (\pi f_{7/2})^5(\nu p_{3/2})$ , changing a  $p_{3/2}$  neutron into a  $f_{7/2}$  proton. In contrast, the  $\text{Fe} \rightarrow \text{Mn}$  would involve  $(\pi f_{7/2})^6 \rightarrow (\pi f_{7/2})^5(\nu p_{3/2})$ , changing a  $f_{7/2}$  proton into a  $p_{3/2}$  neutron. Using the above naive assignments, we are led to the conclusion that the  $\beta^-$  form factor should be about  $\sqrt{3}$  times larger than the  $\beta^+$  form factor. Even though the detailed shell model results are not fully determined by the indicated single particle transitions (but they are the largest ones), the overall scaling factor emerges.

Among the  $sd$  shell transitions in Table I, the transition to the 1.8 MeV state in  $^{26}\text{Mg}$  agrees perfectly with the experiment, while the calculated form factors for the other two are somewhat larger, by a factor of about 1.5, than the experimental value. For  $^{10}\text{Be}$  decay the calculated form factor is also a bit larger. We cannot, therefore, draw any conclusion about the necessity of quenching in the case of the unique second forbidden transitions. While the lighter  $p$  and  $sd$  shell nuclei contain perhaps a hint that quenching is needed, it would obviously spoil the agreement in the case of the  $\beta^+$  branch of the  $^{54}\text{Mn}$  decay.

In conclusion, our shell model calculations reproduce the experimental half-lives of the unique second forbidden beta decays within a factor of less than 2. No clear evidence for the quenching of the corresponding form factors emerges. For the stripped  $^{54}\text{Mn}$  decays, the shell model describes the  $\beta^+$  branch within errors. It predicts that the form factor for the  $\beta^-$  decay is larger than the one for the  $\beta^+$  decay. The calculated  $\beta^-$  half-life (and therefore also the total half-life) is noticeably shorter than the range based on the observation of  $^{54}\text{Mn}$  in cosmic rays. This conflict, albeit relatively mild, makes attempts to determine the branching ratio for the  $\beta^-$  decay experimentally even more compelling.

TABLE I. Form factors and half-lives for the  $\beta^+$  and  $\beta^-$  unique second-forbidden transitions.

	$R^2 A F_{321}^0$ (fm $^2$ )			Half-life (years)		
	HO	Woods-Saxon	Expt	HO	Woods-Saxon	Expt
$^{54}\text{Mn}(\beta^+)^{54}\text{Cr}$	7.82	7.76	$7.1 \pm 0.7$	$5.55 \times 10^8$	$5.64 \times 10^8$	$(6.7 \pm 1.3) \times 10^8$
$^{54}\text{Mn}(\beta^-)^{54}\text{Fe}$	11.7	11.6		$4.89 \times 10^5$	$4.98 \times 10^5$	
$^{22}\text{Na}(\beta^+)^{22}\text{Ne}$	9.24	9.78	$6.0 \pm 0.8$	$2.04 \times 10^3$	$1.87 \times 10^3$	$(4.8 \pm 1.3) \times 10^3$
$^{26}\text{Al}(\beta^+)^{26}\text{Mg}^a$	2.44	2.78	$2.38 \pm 0.05$	$8.64 \times 10^5$	$6.65 \times 10^5$	$(9.1 \pm 0.4) \times 10^5$
$^{26}\text{Al}(\text{EC})^{26}\text{Mg}^a$	2.44	2.78	$2.39 \pm 0.05$	$4.58 \times 10^6$	$3.52 \times 10^6$	$(4.8 \pm 0.2) \times 10^6$
$^{26}\text{Al}(\text{EC})^{26}\text{Mg}^b$	12.6	13.8	$8.8 \pm 0.5$	$1.43 \times 10^7$	$9.44 \times 10^6$	$(2.7 \pm 0.3) \times 10^7$
$^{10}\text{Be}(\beta^-)^{10}\text{B}$	23.1	23.3	$20.4 \pm 0.4$	$1.18 \times 10^6$	$1.16 \times 10^6$	$(1.51 \pm 0.06) \times 10^6$

<sup>a</sup>The first-excited state at 1.809 MeV in  $^{26}\text{Mg}$ .

<sup>b</sup>The second-excited state at 2.938 MeV in  $^{26}\text{Mg}$ .

P. V. is supported in part by the U.S. Department of Energy under Grant No. DE-FG03-88ER-40397. G. M. P. is supported in part by the DGICYES (Spain). Computational resources were provided by the Center for Advanced Computational Research at Caltech.

- 
- [1] M. A. DuVernois, Phys. Rev. C **54**, R2134 (1996).  
[2] M. A. DuVernois, Astrophys. J. **481**, 241 (1997).  
[3] J. A. Simpson, Annu. Rev. Nucl. Part. Sci. **33**, 323 (1983).  
[4] J. E. Grove, B. T. Hayes, R. A. Mewaldt, and W. R. Weber, Astrophys. J. **377**, 680 (1991).  
[5] R. A. Leske, Astrophys. J. **405**, 567 (1993).  
[6] K. Zaerpoor *et al.*, Phys. Rev. Lett. **79**, 4306 (1997).  
[7] A. H. Wuosmaa *et al.*, Phys. Rev. Lett. **80**, 2085 (1998).  
[8] Huo Junde, Nucl. Data Sheets **68**, 887 (1993). Data extracted using the NNDC On-Line Data Service from the ENSDF database, revision March 6, 1998.  
[9] E. K. Warburton, G. T. Garvey, and I. S. Towner, Ann. Phys. (N.Y.) **57**, 174 (1970).  
[10] F. Ajzenberg-Selove, Nucl. Phys. **A490**, 1 (1988). Data extracted using the NNDC On-Line Data Service from the ENSDF database, revision March 6, 1998.  
[11] P. M. Endt, Nucl. Phys. **A521**, 1 (1990). Data extracted using the NNDC On-Line Data Service from the ENSDF database, revision March 6, 1998.  
[12] H. Behrens and J. Jänecke, in *Numerical Tables for Beta Decay and Electron Capture*, Landolt-Börnstein, New Series, Vol. I/4 (Springer, Berlin, 1969).  
[13] A. R. Edmons, *Angular Momentum in Quantum Mechanics* (Princeton University Press, Princeton, New Jersey, 1960).  
[14] I. S. Towner and J. C. Hardy, in *Symmetries and Fundamental Interactions in Nuclei*, edited by Wick C. Haxton and Ernest M. Henley (World Scientific, Singapore, 1995).  
[15] A. Poves and A. P. Zuker, Phys. Rep. **70**, 235 (1981).  
[16] E. Caurier, code ANTOINE, Strasbourg, 1989.  
[17] E. Caurier, G. Martínez-Pinedo, A. Poves, and A. P. Zuker, Phys. Rev. C **52**, R1736 (1995).  
[18] E. Caurier, A. Poves, and A. P. Zuker, Phys. Rev. Lett. **74**, 1517 (1995).  
[19] I. S. Towner, J. C. Hardy, and M. Harvey, Nucl. Phys. A **284**, 269 (1977).  
[20] H. de Vries, C. W. de Jager, and C. de Vries, At. Data Nucl. Data Tables **36**, 495 (1987).  
[21] A. Bohr and B. R. Mottelson, *Nuclear Structure* (Benjamin, New York, 1969), Vol. I.  
[22] B. H. Wildenthal, Prog. Part. Nucl. Phys. **11**, 5 (1984).